



Title	The crystal structure of uytенbogaardtite, Ag_3AuS_2 , and its relationships with gold and silver sulfides-selenides
Authors	Bindi, L; Stanley, CJ; Seryotkin, YV; Bakakin, VR; Pal'yanova, GA; Kokh, KA
Description	The file attached is the Accepted/final draft post-refereeing version of the article.
Date Submitted	2017-03-30

1237R – revised version

**The crystal structure of uytenbogaardtite, Ag₃AuS₂, and its relationships
with gold and silver sulfides-selenides**

LUCA BINDI^{1,*}, CHRISTOPHER J. STANLEY², YURI V. SERYOTKIN^{3,4}, VLADIMIR V. BAKAKIN⁵,
GALINA A. PAL'YANOVA^{3,4}, KONSTANTIN A. KOKH^{3,4}

¹*Dipartimento di Scienze della Terra, Università di Firenze, Via G. La Pira 4, I-50121 Firenze, Italy*

²*Natural History Museum, Cromwell Road, London SW7 5BD, United Kingdom*

³*Sobolev Institute of Geology and Mineralogy of the Siberian Branch of the Russian Academy of Sciences, pr.
Akademika Koptyuga, 3, Novosibirsk 630090, Russia*

⁴*Novosibirsk State University, Pirogova str., 2, Novosibirsk 630090, Russia*

⁵*Institute of Inorganic Chemistry, Siberian Branch of the RAS, prosp. Lavrentieva 3, 630090 Novosibirsk, Russia*

* e-mail address: luca.bindi@unifi.it

Abstract

The crystal structure of the mineral uytenbogaardtite, a rare silver-gold sulfide, was solved using intensity data collected on a crystal from the type locality, the Comstock lode, Storey County, Nevada (U.S.A.). The study revealed that the structure is trigonal, space group $R\bar{3}c$, with cell parameters: $a = 13.6952(5)$, $c = 17.0912(8)$ Å, and $V = 2776.1(2)$ Å³. The refinement of an anisotropic model led to an R index of 0.0140 for 1099 independent reflections. The structure consists of a sublattice of sulfur atoms forming a distorted body-centered cubic arrangement. The structure contains distinct tri-atomic linear groups (S–Au–S) and Ag atoms bonded to four S atoms (from four different linear groups) in a distorted tetrahedral arrangement. On the basis of information gained from this characterization, uytenbogaardtite is here definitively proved to be structurally different from petzite, Ag₃AuTe₂, and fischesserite, Ag₃AuSe₂. By means of high-quality single-crystal diffraction data, the



29 symmetry of the mineral was found to be trigonal, and not tetragonal as erroneously
30 supposed. A revaluation of the powder diffraction data listed in the scientific literature for
31 uytenbogaardtite according to the structural results obtained here leads to an excellent
32 agreement. Crystal-chemical features of uytenbogaardtite, Au_2S , petrovskaitite AgAuS ,
33 uytenbogaardtite–fischesserite series $\text{Ag}_3\text{Au}(\text{S}_{2-x}\text{Se}_x)$ and acanthite–naummanite series
34 $\text{Ag}_2(\text{S}_{1-x}\text{Se}_x)$ are compared.

35

36 **Keywords:** Crystal structure and symmetry; silver sulfides; gold sulfides; minerals;
37 uytenbogaardtite.

38

39 **Introduction**

40 Uytenbogaardtite was defined as a new mineral species by Barton *et al.* (1978) during a
41 study of the ores coming from three different regions: the Tambang Sawah, Benkoelen
42 district, Sumatra (Indonesia), the Comstock lode, Storey County, Nevada (U.S.A.), and
43 Zmeinigorsk, Altai, Russia. The mineral was found to form fine intergrowths with acanthite
44 and electrum. An X-ray single-crystal study was not attempted by Barton *et al.* (1978) owing
45 to the paucity of the mineral, and their structural study was limited to a low-quality X-ray
46 powder investigation made difficult by the several coexisting phases in the selected material
47 for the experiment. Barton *et al.* (1978) assigned a tetragonal cell of $a = 9.76$, $c = 9.78$ Å
48 (Comstock lode), and $a = 9.68$, $c = 9.81$ Å (Tambang Sawah) to uytenbogaardtite, in relation
49 with the studies done previously by Graf (1968) on the synthetic analogue.

50 Messien *et al.* (1966) reported the low-temperature Ag_3AuS_2 to be cubic, $a = 9.72$ Å,
51 but Graf (1968) later argued that the symmetry is actually tetragonal. Observed reflections
52 suggested a primitive space group with the only possible non-unit translational symmetry
53 elements being 4₁- or a 4₃-axis (Graf, 1968). This author also pointed out that given the fact

54 that not many 00 l reflections were observed it is not possible to ascertain with confidence if a
55 four-fold screw axis is present with the probable space group being either $P4_122$ or $P4_1$.

56 Recently, Seryotkin *et al.* (2011) solved the crystal structure of synthetic Ag_3AuS_2 and
57 found that the compound is actually trigonal, space group $R\bar{3}c$. These authors compared the
58 trigonal structure of Ag_3AuS_2 with that of cubic petzite (Ag_3AuTe_2) and fischesserite
59 (Ag_3AuSe_2) and found that it cannot be attributed to the petzite group, because it exhibits a
60 new structure type. By means of the synthesis and structural characterization of gold-silver
61 sulfoselenides belonging to the $\text{Ag}_3\text{Au}(\text{Se,S})_2$ series (i.e., $\text{Ag}_3\text{AuSe}_{1.5}\text{S}_{0.5}$, Ag_3AuSeS , and
62 $\text{Ag}_3\text{AuSe}_{0.5}\text{S}_{1.5}$), Seryotkin *et al.* (2013a and references therein) proved the existence of two
63 solid-solution series: petzite-type cubic Ag_3AuSe_2 – Ag_3AuSeS (space group $I4_132$) and
64 trigonal $\text{Ag}_3\text{AuSe}_{0.5}\text{S}_{1.5}$ – Ag_3AuS_2 (space group $R\bar{3}c$). Both crystal structures differ in the
65 distribution of Ag^+/Au^+ cations in distorted body-centered cubic sublattices of S/Se anions.
66 The morphotropic transformation results from the shrinkage of anion packing accompanied
67 by the shortening of Ag–Ag distances with increase of S content.

68 In the course of a research project dealing with the description and structural
69 characterization of natural silver and gold chalcogenides (Bindi 2008, 2009; Bindi and
70 Cipriani, 2004a, 2004b; Bindi and Pingitore, 2013; Bindi *et al.*, 2004, 2009, 2015), a fragment
71 from the type locality (Comstock lode, Nevada) belonging to the mineralogical collections of
72 the Natural History Museum of London (catalogue number E.1069, off BM 1983, 353) has
73 been examined. Microscopic observations revealed that the sample consists of tiny
74 uytenbogaardtite grains cut by veinlets of acanthite with gangue minerals of calcite and
75 quartz.

76 To help resolve the concerns relating to the structure of uytenbogaardtite, new crystal
77 structure data for the mineral from its type locality are presented here. We show that the

78 structure of uytenbogaardtite mineral, earlier incorrectly interpreted as having a tetragonal
79 cell, is identical to that of the synthetic trigonal Ag_3AuS_2 end-member.

80

81 **X-ray crystallography**

82 A small crystal fragment ($55 \times 61 \times 72 \mu\text{m}$) was selected for the single-crystal X-ray
83 diffraction study. The intensity data collection (see Table 1 for details) was carried out by
84 means of an Oxford Diffraction Xcalibur 3 single-crystal diffractometer (X-ray radiation
85 $\text{MoK}\alpha$, $\lambda = 0.71073 \text{ \AA}$) fitted with a Sapphire 2 CCD detector. A total of 714 frames of data
86 were collected at room temperature as 7 sets of omega runs with an exposure time of 80 s per
87 frame and a frame width of 1.00° . This afforded an overall data collection of 47568
88 reflections (1099 unique). The refined unit-cell parameters are $a = 13.6952(5)$, $c = 17.0912(8)$
89 \AA , and $V = 2776.1(2) \text{ \AA}^3$, which are in a very good agreement with those found by Seryotkin
90 *et al.* (2011) [$a = 13.7104(4) \text{ \AA}$, $c = 17.1170(6) \text{ \AA}$, and $V = 2786.5(2) \text{ \AA}^3$] for the synthetic
91 Ag_3AuS_2 .

92 Data frames were processed using the *CrysAlis* software package (Oxford Diffraction,
93 2006) running on the Xcalibur 3 control PC. The program ABSPACK (Oxford Diffraction,
94 2006) was used for the absorption correction. The merging R for the data set decreased from
95 0.114 before the absorption correction to 0.032 after this correction. The observed reflection
96 conditions, together with the statistical tests on the distribution of $|E|$ values that strongly
97 indicated the presence of an inversion centre ($|E^2 - 1| = 0.957$) and the indications from the
98 previous structure solution by Seryotkin *et al.* (2011), pointed unequivocally to the choice of
99 the space group $R\bar{3}c$. The structure solution was then initiated in this space group. The
100 positions of the atoms were determined by means of direct methods (Sheldrick, 2008). The
101 program SHELXL (Sheldrick, 2008) was used for the refinement of the structure. Neutral
102 scattering curves for Ag, Au and S were taken from the *International Tables for X-ray*

103 *Crystallography* (Ibers and Hamilton, 1974). The occupancies of all sites were left free. They
104 were found to be consistent with a full occupation by Ag, Au, and S, respectively, and then
105 fixed. At the last stage, with anisotropic atomic displacement parameters for all atoms and no
106 constraints, the residual value settled at $R = 0.0137$ for 907 observed reflections [$F_o > 4\sigma(F_o)$
107 level] and 38 parameters and at $R = 0.0140$ for all 1099 independent reflections. Inspection of
108 the difference Fourier map revealed that maximum positive and negative peaks were 1.81 and
109 $1.78 \text{ e}^-/\text{\AA}^3$, respectively. Experimental details and R indices are given in Table 1. Fractional
110 atomic coordinates and anisotropic displacement parameters are reported in Table 2. Structure
111 factors are deposited with the Principal Editor of Mineralogical Magazine at
112 http://www.minersoc.org/pages/e_journals/dep_mat.html. Bond distances are reported in
113 Table 3.

114

115 **Optical properties**

116 Qualitative observations of uytenbogaardtite in plane polarized reflected light are
117 broadly in agreement with those of Barton *et al.* (1978). Under low power microscopic
118 examination there is only a subtle difference between different orientations of
119 uytenbogaardtite and the associated acanthite, both appearing a slightly bluish-grey against
120 the dark grey gangue minerals calcite and quartz in association with pyrite (Fig. 1). However,
121 observations using higher magnification objectives show that uytenbogaardtite is distinctly
122 pleochroic in shades of slightly pinkish grey to slightly higher reflecting greenish grey against
123 cross-cutting veins of acanthite (Fig. 2a). Moreover, at such higher magnification the mineral
124 is distinctly light sensitive. For this reason, fully quantitative reflectance measurements were
125 not made as the length of time taken to make measurements exceeded the period of relative
126 stability prior to reaction and spotting of the uytenbogaardtite surface became obvious.

127 It was observed during the light sensitivity reaction that orientations closer to R_o the
 128 basal section in uniaxial minerals, were more susceptible and hence more reactive presumably
 129 because electrons in the conduction band in this orientation are more easily excited by
 130 photons (Fig. 2b). In Figure 2 the slightly higher reflecting greenish grey orientation of
 131 uytenbogaardtite on the right of the image is close to R_o , while the slightly pinkish grey
 132 orientation is probably close to R_e . Since $R_o > R_e$ the mineral is uniaxial negative. In partially
 133 crossed polars, anisotropic rotation tints determined on the latter (Fig. 3) are from a pale green
 134 to deep purple.

135

136

137

Results and Discussion

138

Crystal structure of uytenbogaardtite

139

140

141

142

143

144

In the crystal structure of uytenbogaardtite, the Ag atoms are located in two crystallographically non-equivalent general positions. The four S atoms around each silver atom form an irregular tetrahedron. The Au atoms occupy also two crystallographically non-equivalent positions. Each of them is coordinated by two S atoms at a distance of 2.33–2.37 Å at an S–Au–S angle of $\approx 180^\circ$; in addition, each Au atom has six Ag atoms as its neighbors at a distance of 2.90–3.14 Å.

145

146

147

148

149

150

151

152

The structure may be described on the basis of infinite columns of edge-sharing $[\text{AgS}_4]$ sphenoids additionally connected by $[\text{AuS}_2]$ coordinations situated along threefold symmetry axes (Fig. 4). The crystal-chemical formula of uytenbogaardtite is $^{[4]}\text{Ag}_{12} (^{[2]}\text{Au}^{(7)}\text{S}_2)(^{[2n]}\text{Au}^{(7)}\text{S}_2)_3$ where the coordination number of a cation is enclosed in square brackets and that of an anion in parentheses. The building unit of the column, $\text{Ag}_{12}\text{Au}_4\text{S}_{20}$, consists of four S–Au–S linear groups (one of them lies on the column axis) and 2×6 Ag-tetrahedra (Fig. 4b). Multiplication of the building units by c symmetry plane forms the columns of uytenbogaardtite. The building units are joined in columns via six S^{2-} anions.

153 Columns mutually joined by shared edges of Ag-tetrahedra are multiplied by base translations
 154 of rhombohedral lattice.

155 There are two types of S–Au–S complexes: strictly linear located along the column axis
 156 and slightly bent (indicated as “2n” (Lima-de-Faria *et al.*, 1990)) with the angle (S–^[2n]Au–S)
 157 of 179.35°. The complexes of the second type are located on the periphery of the columns.

158 The structure of the natural uytenbogaardtite is very similar to that of synthetic
 159 compound Ag_{2.94}Au_{1.06}S₂ (Seryotkin *et al.*, 2011), excluding the low-occupied Au₃ site
 160 lacking in the structure of the current mineral sample. This disagreement is explained by the
 161 presence of AgAuS (petrovskaita) inclusion in the synthetic sample. A minor portion of this
 162 compound could affect the crystal data due to a topotactic integrowth of the two structures
 163 with similar anion sublattices (Seryotkin *et al.*, 2014).

164

165 *Comparison with the crystal structures of Au- and Ag-sulfoselenides*

166 Anion sublattice of many chalcogenides in this group is described according to the
 167 body-centered cubic packing (**bcc**) model. Such sublattice may be divided entirely into
 168 distorted tetrahedra or sphenoids (Bakakin, 2011; Seryotkin *et al.*, 2011). A part of sphenoids
 169 are occupied by Ag atoms; Au atoms are situated at the edges of vacant sphenoids. Thus, the
 170 structural features of a given compound are defined by the occupation of sphenoids by cations
 171 and by steric parameters of anions which form the sublattice.

172 The compounds with common formulae (Ag,Au)₂(S,Se) are listed in Table 4. In these
 173 structures the sublattice of S- and Se-atoms forms a distorted (excluding Au₂S) body-centered
 174 cubic arrangement. It should be noticed that normalized volumes V_N (Bakakin and Seryotkin,
 175 2009) are fairly close for the listed compounds (19.3–21.1 Å³).

176 Worthy to note, the grade of distortion of anion sublattice does not relate directly to the
 177 symmetry of compound. The deviation from ideal **bcc** depends on deformation of its two-

178 anionic subcell. Generally, the unit cell comprises several subcells, so the crystal symmetry
 179 depends on their combination. Coincidence of symmetries of anion sublattice and entire
 180 crystal structure was found only for Au₂S ($Z = 2$, Ishikawa *et al.*, 1995) and argentite, high
 181 temperature phase of Ag₂S ($Z = 2$, Cava *et al.*, 1980). In other related structures (Table 4) the
 182 unit cell comprises from 2 (acanthite, naumannite) to 24 (uytenbogaardtite) subcells in anion
 183 sublattice.

184 The compounds containing linear X^{−[2]}M–X groups in the structure have symmetry axis
 185 of third order. Silver chalcogenides without the linear groups are of lower symmetry. The
 186 meaningful example is cubic Au₂S which has only linear groups in the structure. Au⁺ cations
 187 are located collinearly on body diagonals of anion **bcc** cells forming two interpenetrating
 188 three-dimensional networks with S^{2−} in tetrahedral coordination. The anion subsystem
 189 corresponds to ideal body-centered cubic packing.

190 Addition of cation with coordination number > 2 to linearly coordinated Au⁺ results in
 191 the change of bonding system in the chalcogenide structure. Depending on the ratio of cations
 192 with different coordination, the three dimensional network of linear groups transforms to
 193 another configuration or breaks into fragments (chains, rings, single linear groups). For
 194 instance, in orthorhombic NaAuS with **bcc** anion packing the Na⁺ cations in tetrahedral
 195 coordination are joined in a framework, and the ([²ⁿ]Au–S)[∞] chains coil in an unusual fashion
 196 so that they are interwoven to form layers reminiscent of “chicken-wire” (Axtell *et al.*, 1998).

197 Three fourths of Ag⁺ cations form a tetrahedral framework in rhombohedral
 198 petrovskaitite AgAuS. The linear groups S–(Au,Ag)–S form four interpenetrating three-
 199 dimensional networks (Seryotkin *et al.*, 2014). The number of Au cations alone is not enough
 200 to form the networks, so a fourth part of Ag⁺ gained linear coordination. The detailed crystal-
 201 chemical formula of petrovskaitite with cation ratio [²]M:^[4]M = 5:3 may be written as ^[4]Ag₆
 202 [^[2]Ag^[2](Ag_{0.33}Au_{0.67})₃^[2n]Au₆⁽⁶⁾S₆⁽⁴⁾S₂], or simplified ^[4]Ag₃[^[2]Ag^[2]Au₄⁽⁶⁾S₃⁽⁴⁾S]. The sublattice

203 of sulfur anions has a strongly distorted **bcc** arrangement, caused by specific coordination of
 204 S^{2-} . Three fourths of anions are one-side coordinated by two Au^+ and four Ag^+ . The
 205 remaining part has only four neighboring Au^+ forming a regular tetrahedron.

206 Uytendogaardite has a ratio $^{[2]}M:^{[4]}M = 1:3$ and its structure contains only isolated S–
 207 Au–S linear groups. In spite of the different coordination of cations, the deviation of anion
 208 sublattice from the **bcc** arrangement is quite small. All anions have similar coordination,
 209 which is likely to explain with the lower degree of distortion of anion sublattice compared to
 210 petrovskaitite.

211 The structure of cubic fischesserite is composed of secondary building units of the same
 212 topology as in structure of uytendogaardite (Seryotkin *et al.*, 2011). The difference is in the
 213 manner of multiplication of building units in columns. In the uytendogaardite case,
 214 multiplication is realized by means of reflection and a translation shift by the *c* symmetry
 215 plane. In the fischesserite structure, they are multiplied by translation along the body diagonal
 216 without reflection. Both crystal structures differ in the distribution of Ag^+/Au^+ cations. As a
 217 result, **bcc** sublattice of fischesserite is more distorted than that of uytendogaardite.

218 The structure of uytendogaardite tolerates the substitution of up to 40% of sulfur atoms
 219 by selenium. Two solid-solution Ag_3AuS_2 – Ag_3AuSe_2 series exist: trigonal uytendogaardite-
 220 like Ag_3AuS_2 – $Ag_3AuSe_{0.75}S_{1.25}$ and cubic fischesserite-like Ag_3AuSeS – Ag_3AuSe_2 (Seryotkin
 221 *et al.*, 2013a,b). The morphotropic transformation between the two structure types results
 222 from the shrinkage of anion packing accompanied by the shortening of Ag–Ag distances. It is
 223 generally assumed that the Ag–Ag interactions help to stabilize the structures of Ag–
 224 chalcogenides (Makovicky, 2006). However, the stabilizing effect of such interaction is
 225 limited to a certain range of interatomic distances, and an excessive shortening may cause
 226 instability of the crystal structure. For instance the S–S distances in the pseudocubic
 227 arrangement in uytendogaardite vary in the range 3.81–4.74 Å with a mean value of 4.22 Å,

228 whereas the range observed in fischesserite is 3.43–5.20 Å, with a mean value of 4.33 Å.
229 Since the Ag–Ag distance is equal to 2.89 Å in metal silver (Spreadborough and Christian,
230 1959), it can be assumed that the approach to this value is critical. Probably the same
231 interaction causing destabilization of the fischesserite-like crystal structure causes the
232 morphotropic transformation. Indeed, the shortest Ag–Ag bonds in Ag₃AuSSe and
233 Ag₃AuS_{1.5}Se_{0.5} are equal to 2.99 and 3.01 Å, respectively, whereas the calculated value for the
234 model petzite-like structure of Ag₃AuS₂ is 2.93 Å (Seryotkin *et al.*, 2013a).

235 The morphotropic transition of the same nature may be found in another chalcogenide
236 series between acanthite Ag₂S (Frueh, 1958) and naummanite Ag₂Se (Pingitore *et al.*, 1992;
237 Seryotkin *et al.*, 2015). The compounds have distorted anion **bcc** arrangement with Ag⁺ in
238 planar ternary and distorted tetrahedral coordinations. Interestingly, the distortion of **bcc**
239 arrangement is lower in monoclinic acanthite than in orthorhombic naumannite. There are
240 short Ag–Ag distances ranging in the interval 2.9–3.0 Å in the structure of naumannite.
241 Partial substitution of selenium by sulfur results in a further shortening of the distances
242 (Seryotkin *et al.*, 2015). In the structure of acanthite Ag₂S the distribution of cations is
243 slightly different and all Ag–Ag distances are ≥ 3.0 Å. This can be considered as a cause of
244 morphotropic transition in this series.

245
246
247

Acknowledgements

248 X-ray intensity data were collected at CRIST, Centro di Cristallografia Strutturale,
249 University of Florence, Italy. This work was funded by “Progetto d’Ateneo 2013” issued to
250 LB. The paper benefited by the official reviews made by Tonči Balić-Žunić, Peter Leverett
251 and Ernst Spiridonov.

252

REFERENCES

253

- 254 Axtell, E.A., Liao, J.H. and Kanatzidis, M.G. (1998) Flux synthesis of LiAuS and NaAuS:
255 “Chicken-wire-like” layer formation by interweaving of (AuS)_nⁿ⁻ threads. Comparison
256 with α -HgS and AAuS (A = K, Rb). *Inorganic Chemistry*, **37**, 5583–5587.
- 257 Bakakin, V.V. (2011) Crystal structures of gold, silver, and sodium chalcogenides:
258 Sphenoidal interpretation. *Crystallography Reports*, **6**, 970–979.
- 259 Bakakin, V.V. and Seryotkin, Yu.V. (2009) Unified formula and volume characteristics in
260 comparative crystal chemistry of natural zeolites. *Journal of Structural Chemistry*, **50**,
261 S116–S123.
- 262 Barton, M.D., Kieft, C., Burke, E.A.J. and Oen, I.S. (1978) Uytendogaardite, a new silver-
263 gold sulfide. *Canadian Mineralogist*, **16**, 651–657.
- 264 Bindi, L. (2008) Commensurate-incommensurate phase transition in muthmannite, AuAgTe₂:
265 First evidence of a modulated structure at low-temperature. *Philosophical Magazine*
266 *Letters*, **88**, 533–541.
- 267 Bindi, L. (2009) Thermal expansion behavior of empressite, AgTe: A structural study by
268 means of in situ high-temperature single-crystal X-ray diffraction. *Journal of Alloys and*
269 *Compounds*, **473**, 262–264.
- 270 Bindi, L. and Cipriani, C. (2004a) Ordered distribution of Au and Ag in the crystal structure
271 of muthmannite, AuAgTe₂, a rare telluride from Sacarîmb, western Romania. *American*
272 *Mineralogist*, **89**, 1505–1509.
- 273 Bindi, L. and Cipriani, C. (2004b) Structural and physical properties of fischesserite, a rare
274 gold-silver selenide from the De Lamar Mine, Owyhee County, Idaho, USA. *Canadian*
275 *Mineralogist*, **42**, 1733–1737.
- 276 Bindi, L. and Pingitore, N.E. (2013) On the symmetry and crystal structure of aguilarite,
277 Ag₄SeS. *Mineralogical Magazine*, **77**, 21–31.

- 278 Bindi, L., Arakcheeva, A. and Chapuis, G. (2009) The role of silver on the stabilization of the
279 incommensurately modulated structure in calaverite, AuTe₂. *American Mineralogist*,
280 **94**, 728–736.
- 281 Bindi, L., Spry, P.G. and Cipriani, C. (2004) Empressite, AgTe, from the Empress-Josephine
282 Mine, Colorado, USA: composition, physical properties and determination of the crystal
283 structure. *American Mineralogist*, **89**, 1043–1047.
- 284 Bindi, L., Stanley, C.J. and Spry, P.G. (2015) Cervelleite, Ag₄TeS: solution and description of
285 the crystal structure. *Mineralogy and Petrology*, **109**, 413–419.
- 286 Cava, R.J., Reidinger, F. and Wuensch, B.J. (1980) Single-crystal neutron diffraction study of
287 the fast-ion conductor β-Ag₂S between 186 and 325°C. *Journal of Solid State*
288 *Chemistry*, **31**, 69–80.
- 289 Frueh, A.J.Jr. (1958) The crystallography of silver sulfide, Ag₂S. *Zeitschrift für*
290 *Kristallographie*, **110**, 136–144.
- 291 Graf, R.B. (1968) The system Ag₃AuS₂-Ag₂S. *American Mineralogist*, **53**, 496–500.
- 292 Ibers, J.A. and Hamilton, W.C. Eds. (1974) *International Tables for X-ray Crystallography*,
293 vol. IV, 366p. Kynock, Dordrecht, The Netherlands.
- 294 Ishikawa, K., Isonaga, T., Wakita, S. and Suzuki, Y. (1995) Structure and electrical properties
295 of Au₂S. *Solid State Ionics*, **79**, 60–66.
- 296 Lima-de-Faria, J., Hellner, E., Liebau, F., Makovicky, E. and Parthe, E. (1990) Nomenclature
297 of inorganic structure types. *Acta Crystallographica*, **A46**, 1–11.
- 298 Makovicky, E. (2006) Crystal structure of sulfides and other chalcogenides. *Reviews in*
299 *Mineralogy and Geochemistry*, **61**, 7–125.
- 300 Messien, P., Baiwir, M. and Tavernier, B. (1966) Structure cristalline du sulfure mixte
301 d'argent et d'or. *Bulletin de la Société Royale des Sciences de Liège*, **56**, 727–733.

- 302 Oxford Diffraction (2006). *CrysAlis* RED (Version 1.171.31.2) and ABSPACK in *CrysAlis*
303 RED. Oxford Diffraction Ltd, Abingdon, Oxfordshire, England.
- 304 Pingitore, N.E., Ponce, B.F., Eastman, M.P., Moreno, F. and Podpora, C. (1992) Solid
305 solutions in the system $\text{Ag}_2\text{S}-\text{Ag}_2\text{Se}$. *Journal of Materials Research*, **7**, 2219–2224.
- 306 Seryotkin, Yu.V., Bakakin, V.V., Pal'yanova, G.A. and Kokh, K.A. (2011) Synthesis and
307 crystal structure of the trigonal silver(I) dithioaurate(I), Ag_3AuS_2 . *Crystal Growth &*
308 *Design*, **11**, 1062–1066.
- 309 Seryotkin, Yu.V., Pal'yanova, G.A., Bakakin, V.V. and Kokh, K.A. (2013a) Synthesis and
310 crystal structure of gold–silver sulfoselenides: morphotropy in the $\text{Ag}_3\text{Au}(\text{Se},\text{S})_2$ series.
311 *Physics and Chemistry of Minerals*, **40**, 229–237.
- 312 Seryotkin, Yu.V., Pal'yanova, G.A. and Savva, N.E. (2013b) Sulfur-selenium isomorphous
313 substitution and morphotropic transition in the $\text{Ag}_3\text{Au}(\text{Se},\text{S})_2$ series. *Russian Geology*
314 *and Geophysics*, **54**, 646–651.
- 315 Seryotkin, Yu.V., Pal'yanova, G.A., Bakakin, V.V. and Kokh, K.A. (2014) Synthesis and
316 crystal structure of silver–gold sulfide AgAuS . Four-fold interpenetrated three-
317 dimensional $[(\text{Au},\text{Ag})_{10}\text{S}_8]$ -networks. *CrystEngComm*, **16**, 1675–1680.
- 318 Seryotkin, Yu.V., Palyanova, G.A. and Kokh K.A. (2015) Sulfur-selenium isomorphous
319 substitution and polymorphism in the $\text{Ag}_2(\text{Se},\text{S})$ series. *Journal of Alloys and*
320 *Compounds*, **639**, 89–93.
- 321 Sheldrick, G.M. (2008) A short history of SHELX. *Acta Crystallographica*, **A64**, 112–122.
- 322 Spreadborough, J. and Christian, J.W. (1959) High-temperature X-ray diffractometer. *Journal*
323 *of Scientific Instruments*, **36**, 116–118.
- 324 Yu, J. and Yun, H. (2011) Reinvestigation of the low-temperature form of Ag_2Se
325 (naumannite) based on single-crystal data. *Acta Crystallographica*, **E67**, i45.
- 326

327

328

329

330

331

332

333

334

FIGURE CAPTIONS

335

Fig. 1. Reflected plane polarized light digital image in air illustrating subtle reflection pleochroism of uyttenbogaardtite from slightly pinkish grey (left) to slightly greenish grey (right). Uyttenbogaardtite is cut by veinlets of acanthite (slightly bluish grey) and the dark grey to black gangue minerals are calcite and quartz. A grain of pyrite gives useful visual reference towards the bottom of the image.

340

341

Fig. 2. Reflected plane polarized light digital image in air illustrating in more detail the relationships between uyttenbogaardtite in different optical orientations and acanthite (a). The grain displaying slightly greenish grey rotation tints on the right of the image is starting to show spotting as a result of light sensitivity after about 30 seconds. (b) As for (a). After about 5 minutes exposure the spotting due to light sensitivity is more obvious particularly on the right hand grain and also at grain boundaries with acanthite.

342

343

344

345

346

347

348

349

Fig. 3. Reflected light digital image with partially crossed polars illustrating the anisotropic rotation tints in the grain on the left as pale green (a) to deep purple (b). The grain on the right approaches isotropy and is close to being a basal section, i.e. R_0 .

350

351

352

353 Fig. 4. The structure of uytenbogaardtite. Projection along c -axis (a). The $\text{Ag}_{12}\text{Au}_4\text{S}_{20}$

354 building units seen from the top and their joining into column along three-fold

355 symmetry axis seen from the side (b).

356

357

TABLE 1. Data and experimental details for the selected uytenbogaardtite crystal

Crystal data	
Formula	Ag ₃ AuS ₂
Crystal size (mm)	0.055 × 0.061 × 0.072
Form	block
Colour	black
Crystal system	Trigonal (hexagonal setting)
Space group	$R\bar{3}c$
<i>a</i> (Å)	13.6952(5)
<i>c</i> (Å)	17.0912(8)
<i>V</i> (Å ³)	2776.1(2)
<i>Z</i>	24
Data collection	
Instrument	Oxford Diffraction Xcalibur 3
Radiation type	MoKα (λ = 0.71073 Å)
Temperature (K)	293(2)
Detector to sample distance (cm)	6
Number of frames	714
Measuring time (s)	80
Maximum covered 2θ (°)	69.96
Absorption correction	multi-scan (ABSPACK; Oxford Diffraction 2006)
Collected reflections	47568
Unique reflections	1099
Reflections with $F_o > 4 \sigma(F_o)$	907
R_{int}	0.032
Range of <i>h</i> , <i>k</i> , <i>l</i>	-15 ≤ <i>h</i> ≤ 16, -18 ≤ <i>k</i> ≤ 18, -27 ≤ <i>l</i> ≤ 27
Refinement	
Refinement	Full-matrix least squares on F^2
Final $R_1 [F_o > 4 \sigma(F_o)]$	0.0137
Final R_1 (all data)	0.0140
Final wR (all data)	0.0321
Number of least squares parameters	38
Goodness of Fit	0.93
$\Delta\rho_{\text{max}}$ (e Å ⁻³)	1.81
$\Delta\rho_{\text{min}}$ (e Å ⁻³)	-1.78

TABLE 2. Atoms, Wyckoff positions, atom coordinates and atomic displacement parameters (\AA^2) for the selected uytenbogaardtite crystal

atom	Wyckoff	<i>x</i>	<i>y</i>	<i>z</i>	U_{11}	U_{22}	U_{33}	U_{12}	U_{13}	U_{23}	$U_{\text{iso}}^*/U_{\text{eq}}$
Ag1	36 <i>f</i>	0.04631(2)	0.21652(2)	0.33751(1)	0.0157(1)	0.0158(1)	0.01536(9)	0.00789(7)	0.00004(6)	0.00000(6)	0.01558(5)
Ag2	36 <i>f</i>	0.83862(2)	0.04245(2)	0.42398(1)	0.0166(1)	0.0167(1)	0.0164(1)	0.00826(8)	-0.00017(6)	0.00002(6)	0.01658(5)
Au1	6 <i>a</i>	0	0	0.25	0.01502(8)	0.01502(8)	0.0146(1)	0.00751(4)	0	0	0.01486(6)
Au2	18 <i>e</i>	0.75437(1)	0	0.25	0.01646(7)	0.01648(8)	0.01603(6)	0.00824(4)	0.00001(2)	0.00002(4)	0.01632(5)
S1	12 <i>c</i>	0	0	0.3887(1)	0.0217(4)	0.0217(4)	0.0245(6)	0.0108(2)	0	0	0.0226(3)
S2	36 <i>f</i>	0.84379(8)	0.18078(7)	0.30325(5)	0.0241(4)	0.0244(4)	0.0243(4)	0.0122(3)	-0.0002(3)	0.0000(3)	0.0243(2)

TABLE 3. Main interatomic distances (Å) for the selected uytenbogaardtite crystal

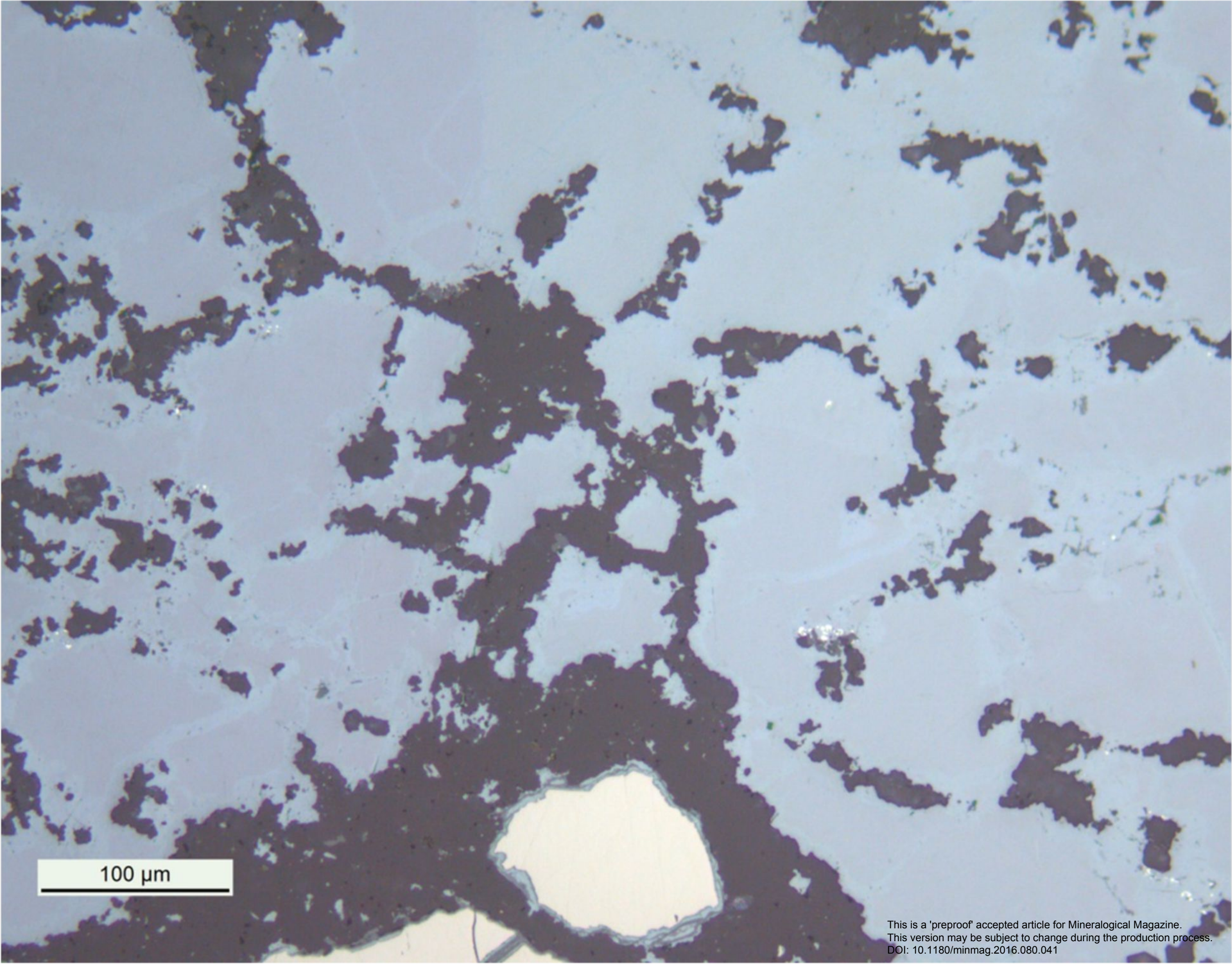
Ag1-S2 ⁱ	2.6301(9)	Au1-S1 ^{xii}	2.370(2)
Ag1-S2 ⁱⁱ	2.8207(9)	Au1-S1	2.370(2)
Ag1-S1	2.8423(6)	Au1-Ag1 ^{xiii}	3.0905(2)
Ag1-S2 ⁱⁱⁱ	2.8795(9)	Au1-Ag1 ^{xii}	3.0905(2)
Ag1-Au2 ^{iv}	2.8998(3)	Au1-Ag1 ^{xiv}	3.0905(2)
Ag1-Au2 ^v	2.9595(2)	Au1-Ag1 ^{xv}	3.0905(2)
Ag1-Ag2 ^v	3.0062(3)	Au1-Ag1 ^{vi}	3.0905(2)
Ag1-Ag2 ⁱ	3.0294(3)	Au1-Au2 ^v	3.3640(2)
Ag1-Au1	3.0905(2)	Au1-Au2 ⁱ	3.3640(2)
Ag1-Ag1 ^{vi}	3.1865(5)	Au1-Au2 ^{xvi}	3.3640(2)
Ag1-Ag1 ^{vii}	3.2523(4)	Au2-S2 ^{xiii}	2.3294(9)
Ag2-S2 ^{viii}	2.546(1)	Au2-S2	2.3294(9)
Ag2-S1 ^{ix}	2.6215(5)	Au2-Ag1 ^{xvii}	2.8998(3)
Ag2-S2 ^x	2.6278(9)	Au2-Ag1 ^{xviii}	2.8999(3)
Ag2-S2	2.7780(9)	Au2-Ag1 ^{xix}	2.9595(2)
Ag2-Ag1 ^{xi}	3.0062(3)	Au2-Ag1 ^{xi}	2.9595(2)
Ag2-Ag1 ^{ix}	3.0294(3)	Au2-Ag2 ^{xiii}	3.1369(3)
Ag2-Ag2 ^{viii}	3.0821(4)	Au2-Au1 ^{ix}	3.3640(2)
Ag2-Au2	3.1369(3)		

Symmetry codes: (i) $x-1, y, z$; (ii) $x-2/3, x-y-1/3, z+1/6$; (iii) $-x+1, -x+y+1, -z+1/2$; (iv) $x-y-2/3, x-1/3, -z+2/3$; (v) $-x+y+1, -x+1, z$; (vi) $-x, -x+y, -z+1/2$; (vii) $-x+1/3, -y+2/3, -z+2/3$; (viii) $y+2/3, x-2/3, -z+5/6$; (ix) $x+1, y, z$; (x) $-x+y+4/3, y-1/3, z+1/6$; (xi) $-y+1, x-y, z$; (xii) $y, x, -z+1/2$; (xiii) $x-y, -y, -z+1/2$; (xiv) $-x+y, -x, z$; (xv) $-y, x-y, z$; (xvi) $-y, x-y-1, z$; (xvii) $y+1/3, -x+y-1/3, -z+2/3$; (xviii) $x+2/3, x-y+1/3, z-1/6$; (xix) $-x+1, -x+y, -z+1/2$.

TABLE 4. Structural characteristics of silver and gold sulfides, sulfoselenides and selenides (Ag,Au)_{2n}(S,Se)_n.

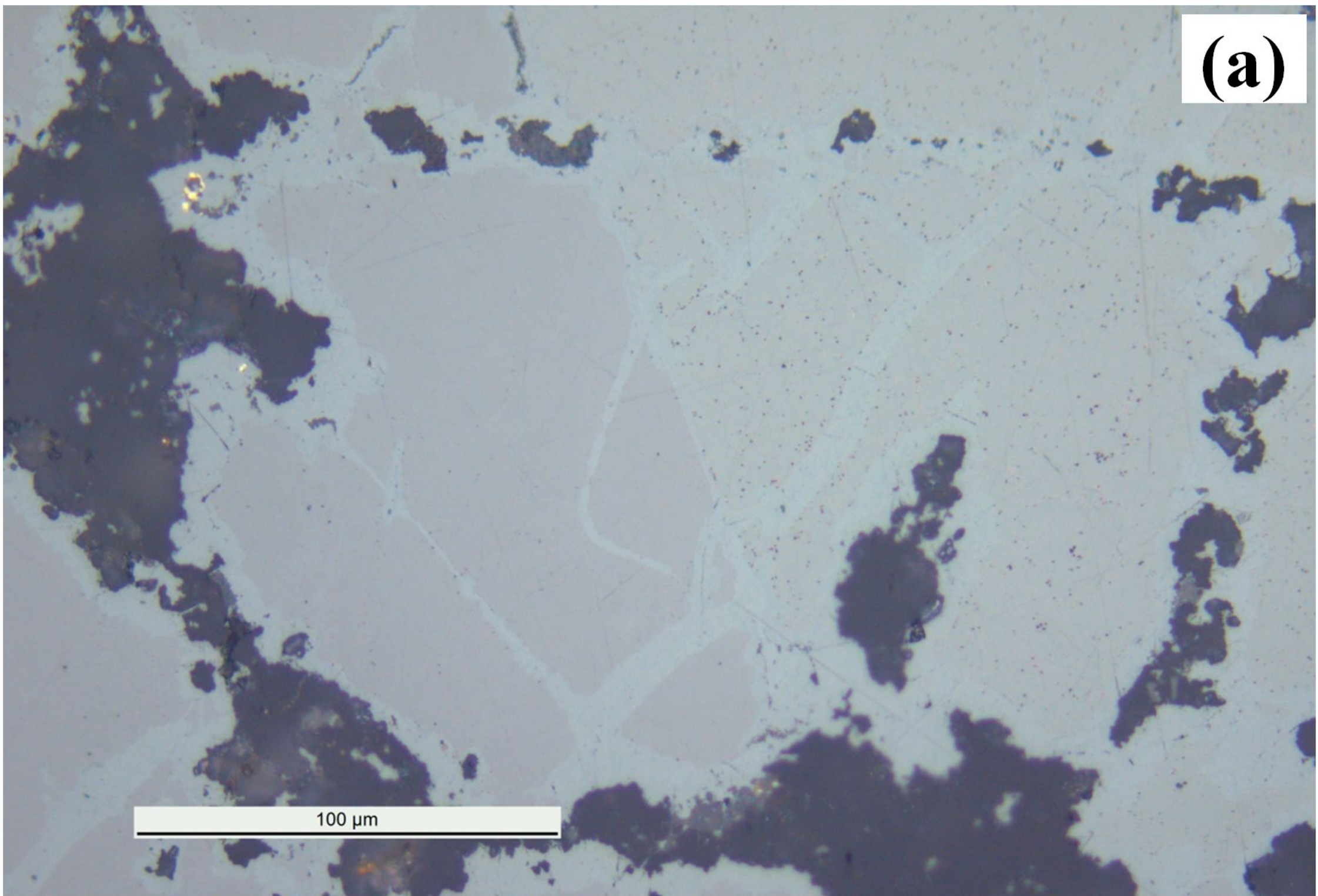
Series	Compound (mineral)	Type	Unit-cell parameters (Å, degrees)				Space group, Z	V_N (Å ³)	Crystal-chemical formula	Reference	
			<i>a</i>	<i>b</i>	<i>c</i>	β					
Ag _{1.5} Au _{0.5} (S _{1-x} Se _x) 0 < x < 1	Au ₂ S	I	5.0206	–	–		<i>Pn</i> $\bar{3}m$, 2	21.1	[² Au ₂ (⁴ S]	Ishikawa <i>et al.</i> (1995)	
	AgAuS (petrovskaitaite)	II	13.4235	–	9.0873		<i>R</i> $\bar{3}m$, 24	19.7	[⁴ Ag ₃ [² Ag ^[2] Au ₄ (⁴ S(⁶ S ₃)]	Seryotkin <i>et al.</i> (2014)	
	Ag ₃ AuS ₂ (uytenbogaardtite)	III	13.6952	–	17.0912		<i>R</i> $\bar{3}c$, 24	19.3		This work	
				13.7104	–	17.1170			19.4	[⁴ Ag ₃ [² Ag ^[2] Au ⁽⁷⁾ S ₂	Seryotkin <i>et al.</i> (2011)
	Ag ₃ Au(S _{1.5} Se _{0.5})	III	13.7752	–	17.2098		<i>R</i> $\bar{3}c$, 24	19.6	[⁴ Ag ₃ [² Ag ^[2] Au ⁽⁷⁾ (S,Se) ₂	Seryotkin <i>et al.</i> (2013a)	
	Ag ₃ Au(S _{1.0} Se _{1.0})	IV	9.8633	–	–		<i>I</i> 4 ₁ 32, 8	20.0	[⁴ Ag ₃ [² Ag ^[2] Au ⁽⁷⁾ (S,Se) ₂	Seryotkin <i>et al.</i> (2013a)	
	Ag ₃ Au(S _{0.5} Se _{1.5})	IV	9.9241	–	–		<i>I</i> 4 ₁ 32, 8	20.4	[⁴ Ag ₃ [² Ag ^[2] Au ⁽⁷⁾ (S,Se) ₂	Seryotkin <i>et al.</i> (2013a)	
Ag ₃ AuSe ₂ (fischesserite)	IV	9.965	–	–		<i>I</i> 4 ₁ 32, 8	20.6	[⁴ Ag ₃ [² Ag ^[2] Au ⁽⁷⁾ Se ₂	Bindi and Cipriani (2004b)		
Ag ₂ (S _{1-x} Se _x) 0 < x < 1	Ag ₂ S (acanthite)	V	4.23	6.91	7.87	99.58	<i>P</i> 2 ₁ / <i>n</i> , 4	18.9	[³⁺¹ Ag ^[2+1] Ag ⁽⁵⁺²⁾ S	Frueh (1958)	
	Ag ₂ (S _{0.5} Se _{0.5}) (aguilarite)	V	4.2478	6.9432	8.0042	100.103	<i>P</i> 2 ₁ / <i>n</i> , 4	19.4	[³⁺¹ Ag ^[2+1] Ag ⁽⁵⁺²⁾ (S,Se)	Bindi and Pingitore (2013)	
	Ag ₂ (S _{0.25} Se _{0.75})	V	4.2716	6.9707	8.1113	100.802	<i>P</i> 2 ₁ / <i>n</i> , 4	19.8	[³⁺¹ Ag ^[2+1] Ag ⁽⁵⁺²⁾ (S,Se)	Seryotkin <i>et al.</i> (2015)	
	Ag ₂ (S _{0.33} Se _{0.67})	VI	4.2845	7.001	7.739		<i>P</i> 2 ₁ 2 ₁ 2 ₁ , 4	19.35	[⁴ Ag ^[3] Ag ⁽⁷⁾ (S,Se)	Seryotkin <i>et al.</i> (2015)	
	Ag ₂ Se (naumannite)	VI	4.3359	7.070	7.774		<i>P</i> 2 ₁ 2 ₁ 2 ₁ , 4	19.9	[⁴ Ag ^[3] Ag ⁽⁷⁾ Se	Yu and Yun (2011)	

Note. Isostructural compounds are shown by same Roman letters.

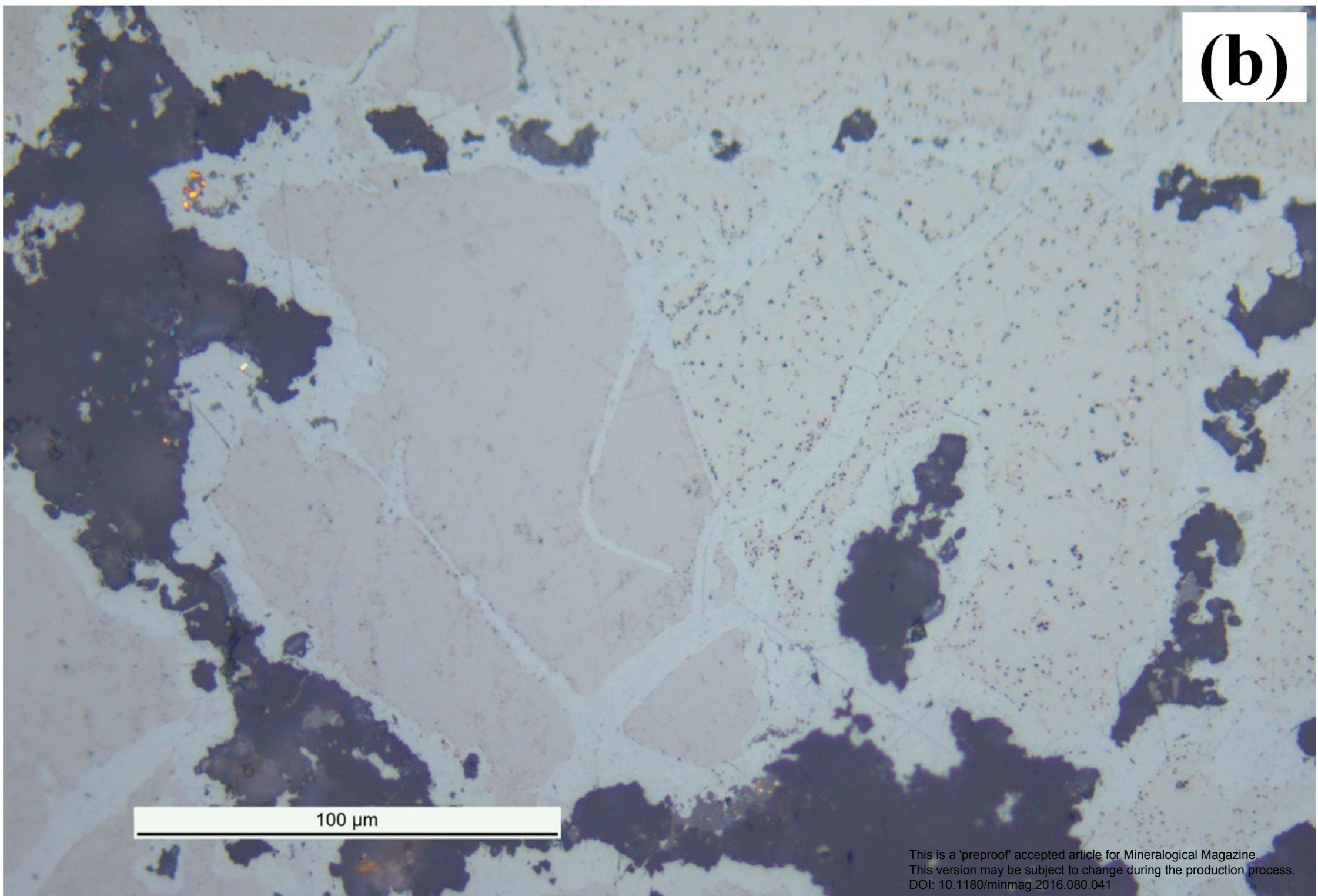


100 μm

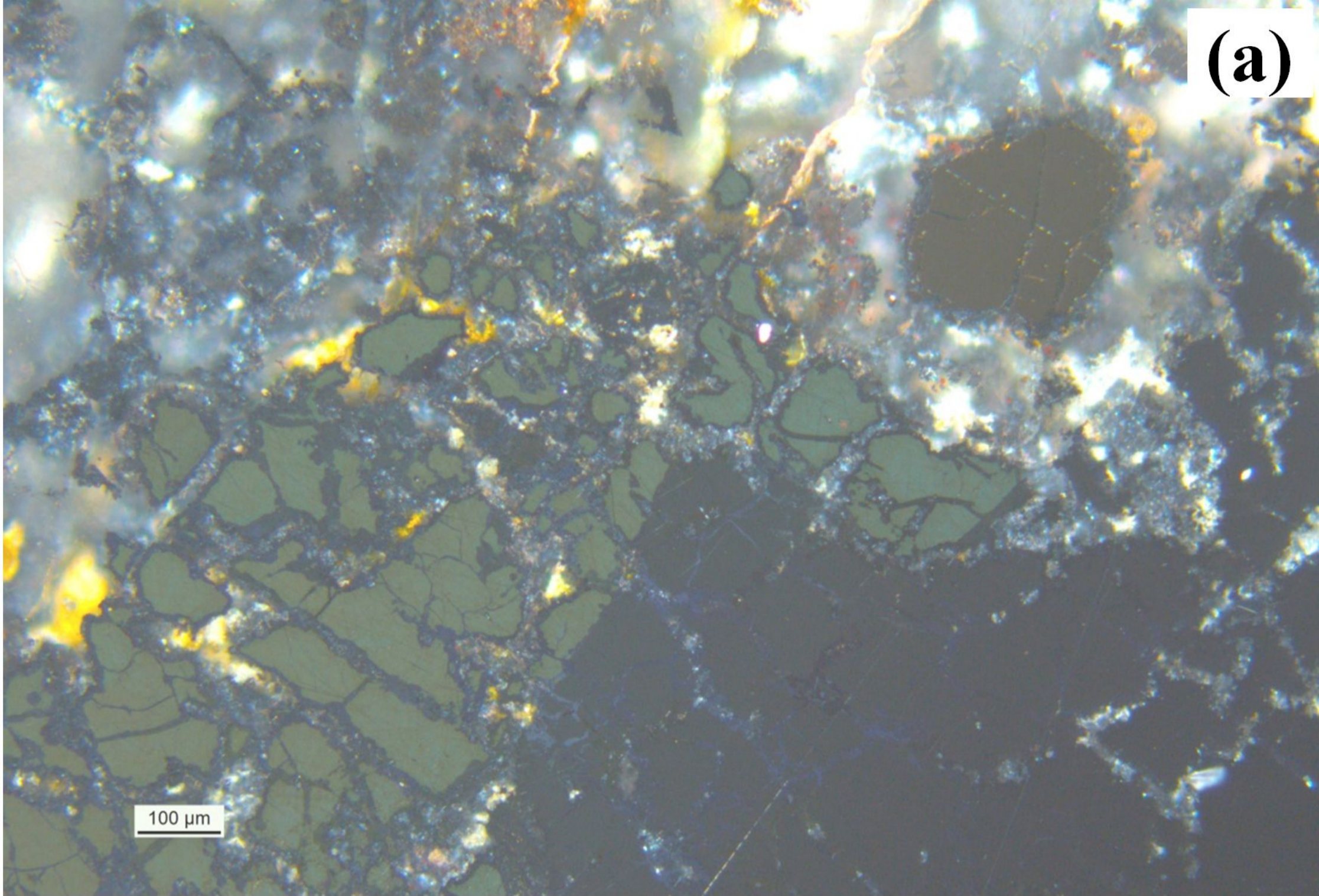
(a)



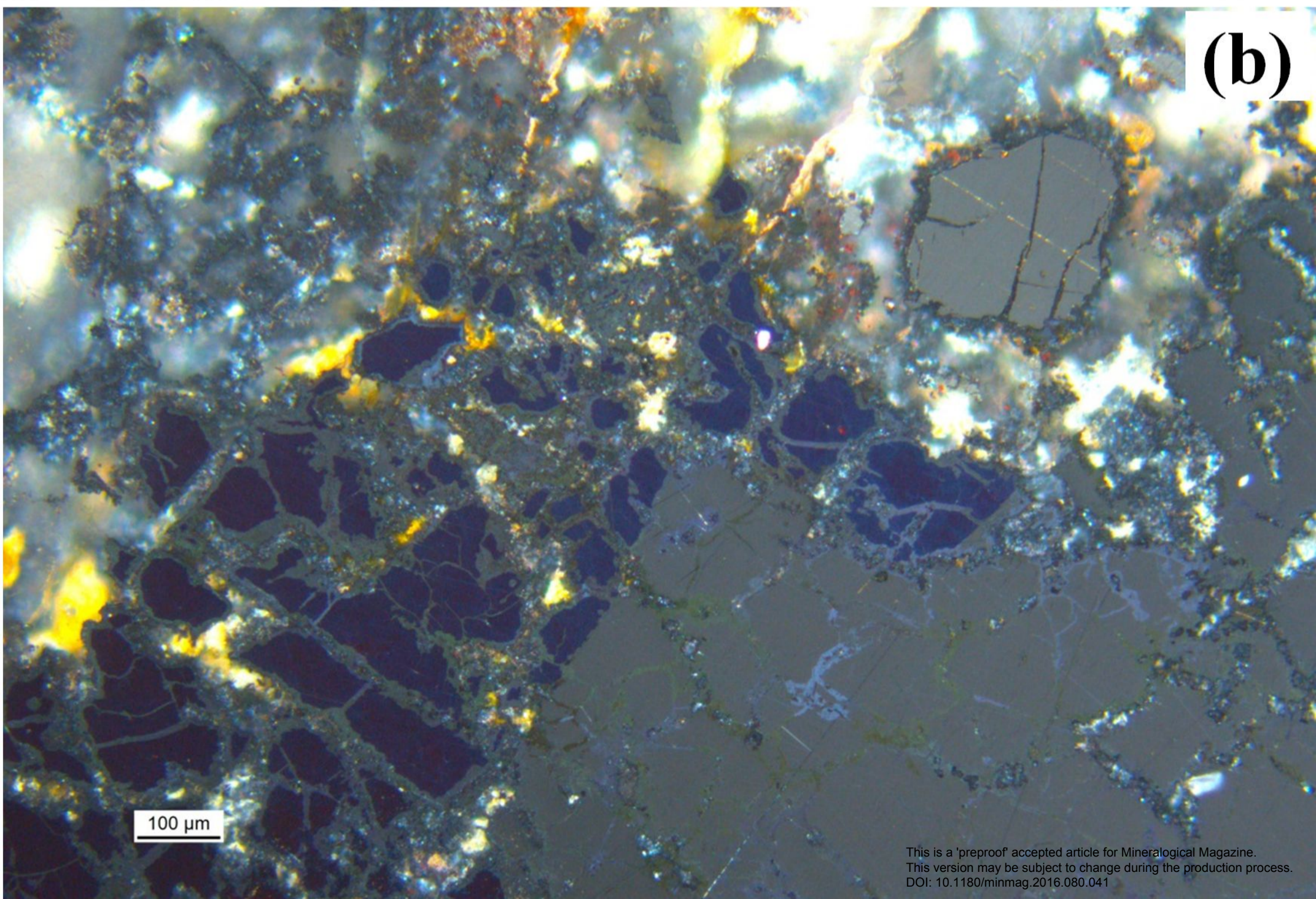
(b)

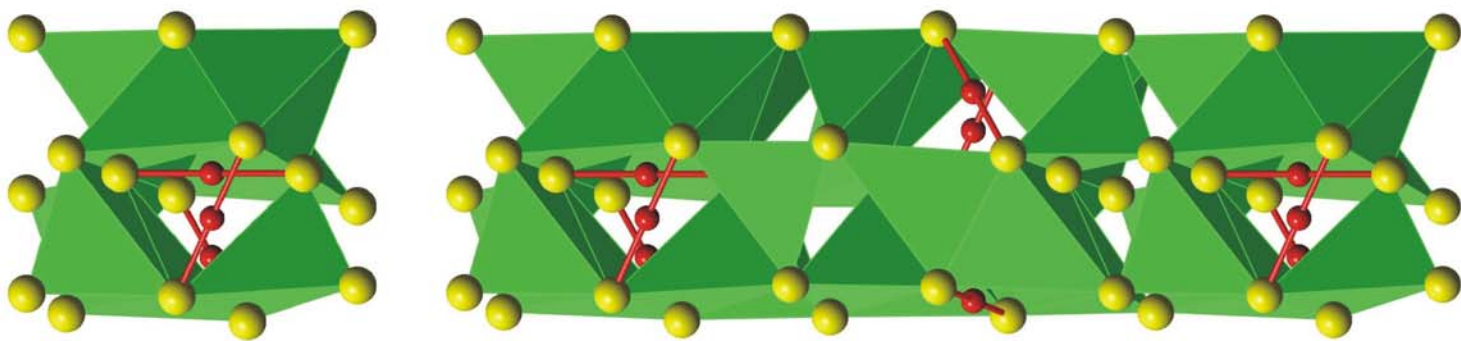


(a)

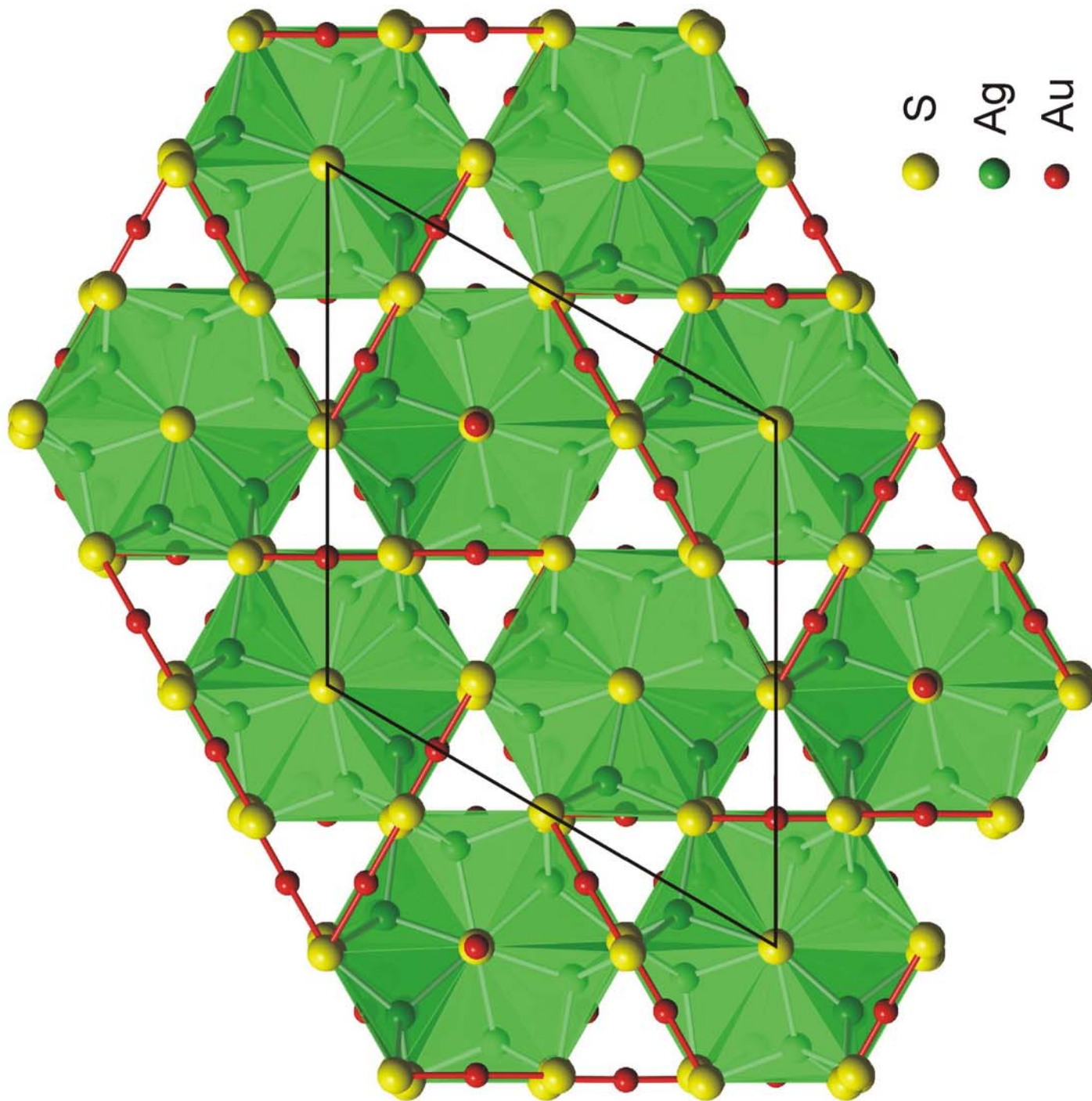


(b)





(b)



(a)